I-1.   PROJECT RESEARCHES

Project 4

PR4　　Chemical and electronic properties of Actinide compounds and their applications

T. Yamamura[1], Y. Haga[2], H. Amitsuka[3], T. Suzuki[4], K. Shirasaki[5], M. Nogami[6], M. Abe[7], H. Shishido[8], M. Nakase[9], H. Nakai[10], T. Kobayashi[11]

[1]*KURNS, Kyoto University*
[2]*Advanced Science Research Center, JAEA*
[3]*Graduate School of Science, Hokkaido University*
[4] *Nagaoka University of Technology*
[5]*Institute for Materials Research, Tohoku University*
[6]*Graduate school of Electronic Eng., Kindai University*
[7]*Department of Chemistry, Tokyo Metropolitan University*
[8]*Graduate School of Engineering, Tohoku University*
[9]*Lab. for Adv. Nuclear Energy, Tokyo Inst. of Tech.*
[10]*Faculty of Science and Engineering, Kindai University*
[11]*Material Science Research Center, JAEA*

INTRODUCTION:

Actinide compounds shows a unique chemical and electronic nature due to the partial and insufficient shield of 5f orbital electrons as inner transition elements. We have a deep interest in the aspect of the electronic properties of the actinide compounds and formed the group consisting of three major fields: (1) inorganic and coordination chemistry, (2) electronic properties and (3) theoretical chemistry and its users. These studies will be also useful for application research area such as the handling of the 1F debris and developments of nuclear medicines.

Such research environments to handle actinides elements are extremely difficult to build in ordinary university institutes. The hot laboratory of the KURNS offers unique opportunities for the above-mentioned characteristic research activities.

EXPERIMENTS:

The last fiscal year of the project has been devoted to the setting up the experimental environment and initial test experiments. Each of research fields has made their progress as followings:

(1) T. Suzuki *et al.* has the investigated adsorption behaviors of actinides on polyvinylpolypyrrolidone (PVPP) in nitric acid and hydrochloric acid solutions. The adsorption behaviors were evaluated through measurements of the distribution coefficient.

(2) Y. Haga *et al*. has synthesized the novel uranium intermetallic compound $U_2Pt_6Ga_{15}$. The single-crystalline samples of this compound have been investigated by the measurements of crystallographic, thermodynamic, and transport properties.

(3) M. Nakase *et al.* has studied properties of Phthalocyanine (Pc) as a ligand for an effective extraction of U. The Pc-Zn complex was sublimely purified in a self-made apparatus that was maintained last year. The pure product was found to be solid (powder), but slightly moistened by moisture in the air. Powder X-ray diffraction (PXRD) and Raman spectrophotometry were used.

(4) Kobayashi *et al.* has studied changes in the chemical state and structure of simulated fuel debris were studied under a controlled environment simulating the environment inside and outside a nuclear reactor were investigated by XAFS. conducted at the JAEA beamline BL22XU at SPring-8.

(5) Abe et al. calculated isotopic fractionation factors (ε) for 64 U(VI), U(V), and U(IV) species with various ligands using an exact relativistic quantum chemistry method. U isotopic fractionation is important and widely discussed in geochemistry [1]. We validated the accuracy of our method by comparing it with experimental results for U isotope fractionation.
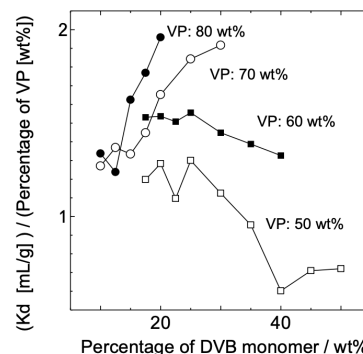

Fig.1 Cross-linkage effects on adsorption of uranyl ion on pyrrolidone resin in HNO_3.

RESULTS:

(1) From the distribution coefficients measured for uranyl ions on PVPP, T. Suzuki *et al.* confirmed that the thorium is strongly adsorbed on PVPP in higher concentration of HNO, and the cross-linkage effects on adsorption of uranyl ion on pyrrolidone resin. They found that this tendency change is related with the surface potential of resin.

(2) Uranium layers embedded in Pt-Al(Ga) metal blocks exhibit a variety of magnetic properties [2]. Although the transition temperatures are almost the same, the behavior at low temperatures is quite different: $U_2Pt_6Ga_{15}$ exhibits typical antiferromagnetic, whereas $U_2Pt_6Al_{15}$ shows a rapid expansion of magnetization in the ordered state.

(3) The purified Pc-Zn sample and its XRD pattern are shown in Fig. 2. the XRD pattern shows a large halo peak due to the use of ethanol and a glass plate, but also some sharp diffraction due to Pc. Therefore, we conclude that the purification by sublimation was successful.

(4) Immersion in water and γ-ray irradiation has found to oxidize uranium on the sample surface from tetravalent to hexavalent and the U-O distance was shortened. No change in uranium valence or local structure was observed when the samples were removed from the water and exposed to atmospheric air, suggesting that the debris may be stable in the air.

(4) Obtained values of ε were almost U(VI)>U(V)>U(IV) for both HF and DFT. The X2C-HF method seems to be more reliable for the calculation between U(VI)-U(IV). On the other hand, when the isotopic fraction of the U(VI)-U(VI) ligand exchange system is considered, the values obtained at the DFT level are generally in better agreement with experiments than the HF values.

REFERENCES:

[1] T. Yamamizu, *et al.*, Jpn. J. Polymer Sci. Technol., 47 (1990)49-56.
[2] Y. Matsumoto, Y. Haga *et al.*, J. Phys. Soc. Jpn. 90, 074707 (2021).

R3P4

PR4-1   Study of Magnetic Structure in UIr$_2$Ge$_2$ by Resonant X-Ray Scattering Experiments

H. Amitsuka, F. Kon, C. Tabata[1], H. Nakao[2], Y. Shimizu[3], D. Aoki[3], A. Koriki, H. Hidaka, and T. Yanagisawa

Graduate School of Science, Hokkaido University
[1]*Institute for Integrated Radiation and Nuclear Science, Kyoto University*
[2]*Institute Materials Structure Science, CMRC, KEK*
[3]*Institure for Materials Research, Tohoku University*

INTRODUCTION: The magnetic structure of the uranium compound UIr$_2$Ge$_2$ has been investigated for the first time by resonant X-ray scattering experiments using a single crystal sample. This compound has a tetragonal CaBe$_2$Ge$_2$-type structure (space group: $P4/nmm$, D_{4h}^7, No. 129) [1,2], which is characterized by an inversion-symmetric pairing of two U ions occupying a site lacking spatial inversion symmetry in the unit cell. When an antiferromagnetic order with order wavenumber $Q = 0$ is induced in such a U ion, the global spatial inversion symmetry of the system is broken and cross-correlated responses such as current-induced magnetization are predicted. For this reason, CaBe$_2$Ge$_2$-type magnetic materials have attracted much attention in recent years because they may provide the simplest example of a system in which odd-parity magnetic multipoles can be active.

On the basis of bulk property measurements on single-crystal sample of UIr$_2$Ge$_2$, we have confirmed that the system exhibits a phase transition suggestive of antiferromagnetic ordering at 18.3 K ($\equiv T_N$), strong magnetic anisotropy with the c-axis as the easy magnetization axis [3]. In the present study, we performed resonant X-ray scattering experiments to identify the magnetic structure of this order.

EXPERIMENTS: The measurements were carried out at BL-11B of KEK PF using soft X-rays of 3.70 ~ 3.75 keV. The sample was a single crystal with a diameter of about 2 mm formed into a plate. The temperature range was 6 K to 24 K. A ^{4}He flow refrigerator was used for cooling.

RESULTS and DISCUSSION: By searching for magnetic reflections in the a^*-c^* plane, it was confirmed that the superlattice reflections due to resonant scattering at the M_4 edge of U ($3d \rightarrow 5f$ transition: 3.723 keV) grow continuously at (reciprocal lattice points) + (0, 0, 1/2) at lower temperatures than near T_N (Fig. 1) [5]. The fact that the magnetic susceptibility of this material shows a cusp anomaly at T_N suggests that an antiferromagnetic ordered state with an ordered wavenumber vector $Q = (0, 0, 1/2)$ is realized below T_N. For the space group $P4/nmm$, there are three maximal magnetic subgroups where the U ion has a magnetic moment and $Q = (0, 0, 1/2)$: $P_{2c}4/nmm$ (No. 129.13.1087), C$_{2c}mma$ (No. 67.11.587), and $P_{2c}mmn$ (No. 59.9.486). Among these, only $P_{2c}4/nmm$ has the magnetic easy axis at c-axis.

In order to identify the direction of the magnetic moment, we measured the azimuth angle dependence of the magnetic scattering intensity. The diffractometer is fixed to the Bragg condition with the magnetic scattering vector $q = (2,$ 0, 1/2), the sample is rotated around q, and the change in scattering intensity is measured. The rotation angle is φ, and the range of $-100° \leq \varphi \leq 90°$ is investigated by setting $\varphi = 0$ so that the (0, 1, 0) direction of the sample is perpendicular to the scattering plane.
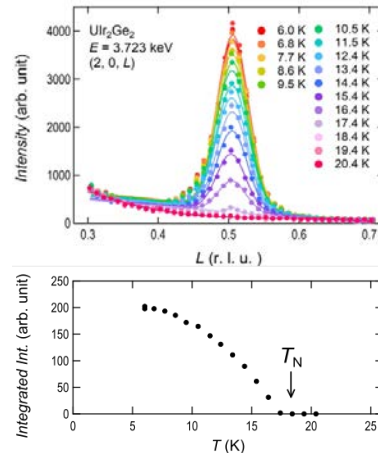

Fig. 1. Temperature profiles of magnetic reflections (2, 0, 1/2) and results of Gaussian-fit (solid line) (top) and temperature dependence of integrated intensity (bottom).

The φ-dependence of the integrated intensity of the magnetic reflections show maxima and minima near $\varphi \sim \pm 90°$ and $\varphi \sim 0$, respectively. The results suggest scattering by magnetic dipoles lying in the c direction, showing a good agreement with calculations based on the magnetic structures belonging to $P_{2c}4/nmm$.

SUMMARY: In this study, we confirmed that the magnetically ordered structure in UIr$_2$Ge$_2$ is antiferromagnetic with $Q = (0, 0, 1/2)$ due to the magnetic dipole parallel to the c-axis. It was found that the system is not an antiferromagnet with $Q = 0$, as expected for the original purpose. However, the ferroicly ordered layers of the odd-parity multipoles may be antiferromagnetically stacked in the c direction due to weak interlayer interactions, which is of interest in relation to a variety of unusual physical properties of this system.

REFERENCES:
[1] B. Lloret *et al.*, J. Magn. Magn. Mater. **67**, 232 (1987).
[2] A. A. Menovsky, J. Magn. Magn. Mater. **76** and **77**, 631 (1988).
[3] F. Kon *et al.*, Physical Society of Japan, Autumn Meeting 2019 (Gifu Univ.), 12pB12-13, September 12, 2019.
[4] A. Bienenstock, J. Appl. Phys. **37**, 1459 (1966).
[5] F. Kon *et al.*, Physical Society of Japan, The 75th Annual Meeting, 16pB22-9, March 2020 (Local meeting cancelled to prevent spread of infection COVID-19).

PR4-2   Balk thorium separation for ^{228}Ac generator

K. Shirasaki, H. Kikunaga[1], K. Washiyama[2], A. Shinohara[3], T. Yoshimura[4], K. Nagata[4], C. Tabata[5], and T. Yamamura[5]

Institute for Materials Research, Tohoku University
[1]*Research Center for Electron Photon Science, Tohoku University*
[2]*Advanced Clinical Research Center, Fukushima Medical University*
[3]*Department of Chemistry, Graduate School of Science, Osaka University*
[4]*Radioisotope Research Center, Institute for Radiation Sciences, Osaka University*
[5]*Institute for Integrated Radiation and Nuclear Science, Kyoto University*

INTRODUCTION: Actinium chelation chemistry has been drawn attention from not only chemists but also medical workers, who are relevant to nuclear medicine. Because ^{225}Ac ($T_{1/2}$ = 10 d) which decays through a chain of four α-emissions and two β-emissions to the stable ^{209}Bi, are of great interest for a targeted alpha therapy nuclide due to its ability to kill considerably high efficiency of tumor cell [1]. However, γ-ray spectrometry, which is a convenient method for identification of radionuclides, has an uncertainty about the application to ^{225}Ac due to its low emission ratios. In contrast, ^{228}Ac ($T_{1/2}$ = 6.15 h, daughter nuclide of ^{228}Ra) has potential value because it emits well-defined and intense γ-rays that are easily resolved from the daughter nuclides. Havelka reported the preparation method of ^{228}Ra standard solution from natural thorium nitrate salt [2]. Aldrich *et al.* also reported the preparation method of ^{228}Ac generator from natural thorium salts in 2020 [3]. Their method was composed of two parts with the balk thorium separation by the precipitation of thorium hydroxide, and purification of ^{228}Ra by the column chromatography using ion-exchange resins. In the handling of thorium hydroxide, the voluminous slurry precipitate complicates the convenient separation from the daughter nuclides.

Hence, we studied precipitation behavior of thorium hydroxide by titration method.

EXPERIMENTS: The precipitation method was based on a technique used in ^{228}Ac separation from natural thorium salts [3]. Thorium oxide (9.95 g) was dissolved in 30 mL of conc. HCl spiked with 0.1 mL of conc. HF with heating (~150°C) for a few minutes. The solution was evaporated near dryness and added mili-Q water (18.2 MΩ, repeated two times). Then, the solution was brought to dryness and dissolved in 0.1 M (mol/L) HCl. Finally, the solution volume was adjusted to 100 mL by the addition of mili-Q water.

The balk thorium separation by NaOH titration was processed according to the following steps. The 20 mL of Th stock solution was diluted to 100 mL with mili-Q water and transferred to a beaker of 250 mL. The solution was intensely stirred and titrated with NaOH solution under pH measuring (Condition A was adjusted to pH12, then reversed by HCl until pH7, refer to previous study [3]: condition B and C were adjusted to pH5 and pH8, respectively.). After the titration, the solution was stayed at several hours (Fig. 1), then the solution passed through a PES filter (0.2 μm filter size). The filtrate was collected, then an additional 20 mL of mili-Q water was passed through for washing the residual (repeated 3 times). These were also corrected in the same bottle. This solution was subjected to the γ-ray spectrometry using a high-pure Ge-detector (ORTEC). The ^{228}Ac activity was determined by γ-emission of 911 keV. The distribution ratio (D) of ^{228}Ra in the solution was calculated by the equation:

$$D = A_{sep}/A_{ini} \qquad (1).$$

Here, A_{sep} and A_{ini} are activities obtained from γ-ray spectrometry of the separated solution and Th stock solution, respectively. Th concentration of the solution was also measured by ICP-AES (ICPS-7500, Shimazu).

RESULTS: As shown in Fig. 1, supernatant liquids were found in Condition A and C, which was assumed to be contained thorium as a major precipitated hydroxide.
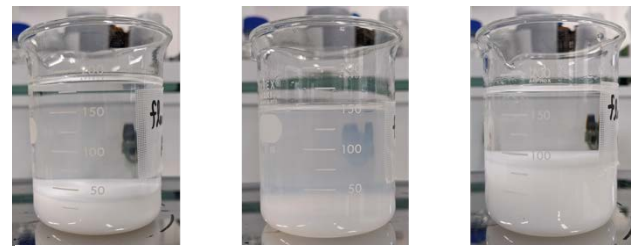
Condition A   Condition B   Condition C

Fig. 1.   photos of titrated samples after titration.

The initial ^{228}Ra atomicity (N_1) of each fraction can be estimated by the equation:

$$N_2' = \lambda_1/(\lambda_2 - \lambda_1) \cdot N_1\left(e^{-\lambda_1 t} - e^{-\lambda_2 t}\right) + N_2 e^{-\lambda_2 t} \quad (2).$$

Here, N_2 and N_2' are the number of ^{228}Ac atom at initial and elapsed time t, respectively, λ_1 and λ_2 are the decay constant of ^{228}Ra and ^{228}Ac, respectively. The distribution ratios (D) of ^{228}Ra in the solutions were determined by ^{228}Ac activities and summarized in Table 1. This result indicates that over 90% of ^{228}Ra is remained in the solution and successful bulk thorium separation is realized in the titration condition both A and C.

Table 1 ^{228}Ra distribution ratio (D) and Th concentration.

Condition no.	A	B*	C
D	0.99	-	0.93
Th conc. (ppm)	5.9	-	< 5.1

*Hard to filtrate the solution

REFERENCES:
[1] C. Kratochwil *et al.*, J. Nucl. Med., **57** (2016) 1941-1944.
[2] M. Havelka, Appl. Rad. Isotopes, **109** (2015) 222-225.
[3] K. E. Aldrich *et al.*, Inorg. Chem., **59** (2020) 3200-3206.

R2P7-4

PR4-3   Elution Properties of Re(VII) from Cyclic Monoamide VBPR Resin by Chelating Agents

M. Nogami[1], N. Mori[1], C. Tabata[2], and T. Yamamura[2]

[1]*Faculty of Science and Engineering, Kindai University*
[2]*Institute for Integrated Radiation and Nuclear Science, Kyoto University*

INTRODUCTION: Development of highly selective compounds for actinyl ions in aqueous media (extractants, precipitants, resins, etc.) has been important. We have been focusing on monoamide compounds (Fig. 1) as promising candidates for nitric acid media, considering the possibility of complete incineration of waste compounds (so-called "CHON principle"[1]). For monoamide resins, not a few have been newly synthesized, and adsorptivity to metal ions has been examined, where uranium(VI) was used as the representative of actinyl ions.

Fig. 1.   Chemical structure of monoamide compounds.
(R, R', R" : hydrocarbon group) .

Effective elution of the adsorbed metal ions is necessary for recycle use of resins. Many of the monoamide resins are found to adsorb more U(VI) species with increasing concentration of HNO_3. Selective U(VI) recovery would be, therefore, achieved by adsorbing U(VI) under relatively higher concentration of HNO_3 (e.g. 3 to 6 mol/dm^3 (=M)) followed by elution of the adsorbed U(VI) by using H_2O or diluted HNO_3 (e.g. 0.1 M). On the other hand, it has been revealed that some metal ions except U(VI) are also adsorbed to monoamide resins. Adsorptivity for many of the ions are lower than that of U(VI), but some ions are adsorbed in almost all HNO_3 concentration range. In this case, the adsorbed metal ions can't be eluted only by changing the concentration of HNO_3, and use of chelating agents is necessary.

In the present study, a monoamide resin consisting of 1-(4-vinylbenzyl)pyrrolidin-2-one (VBPR) was taken. As can be seen in Fig. 2, it has a cyclic monoamide structure with a long spacer between the functional monoamide group and the main polymer chain. VBPR resin shows adsorptivity to Re(VII) (simulant of Tc(VII)) in all HNO_3 concentration range and the distribution ratio, K_d, is higher under lower concentration of HNO_3. Based on the above, elution properties Re(VII) by some chelating agents were investigated.
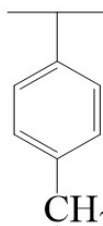

Fig. 2.   Chemical structure of VBPR resin

EXPERIMENTS: VBPR resin is a silica-supported type and was synthesized by following the earlier study[2]. Three chelating agents, ethylenediaminetetraacetic acid tetrasodium salt (EDTA-4Na), oxalic acid (Ox), and trisodium citrate dihydrate (Cit-3Na) were used as the candidate eluents. Elution experiments were carried out by batch method. As the first step, 0.1 M HNO_3 containing 10 mM Re(VII) was mixed with VBPR resin (wet 3.0 g) at 25 ºC for 24 h in order that VBPR resin might adsorb Re(VII). Next the mixture underwent solid-liquid separation. The solid was air-dried and the concentration of Re in HNO_3 was measured by ICP-OES. The dried VBPR resin (0.15 g) was mixed with solutions containing 0.1 M chelating agents mentioned above and H_2O for reference, respectively (3 cm^3 each), at 25 ºC for 24 h. The mixture underwent solid-liquid separation again and the concentration of Re in HNO_3 was measured by ICP-OES. Elution ratios were calculated by the eluted amount of Re divided by the adsorbed one.

RESULTS: Elution ratios of Re(VII) by each chelating agent are shown in Table 1. All examined chelating agents are found to elute Re(VII) more effectively than H_2O. Above all, elution ratio by Cit-3Na is highest. The reason still remains unclear and further investigations are necessary.

Table 1.   Elution ratio of Re(VII)
by each chelating agent.

	EDTA-4Na	Ox	Cit-3Na	H_2O
Elution ratio / %	7.8	24.4	32.6	3.6

Following the above result, dependence of Cit-3Na concentration on elution ratio was examined. The result is shown in Fig. 3. The data for H_2O in Table 1 is used for [Cit-3Na] = 0 M. The elution ratio is increased with increasing concentration of Cit-3Na up to 0.1 M and almost constant over 0.1 M. This suggests that ca. 0.1 M is the most appropriate concentration of Cit-3Na for eluting Re(VII) under the present experimental condition.
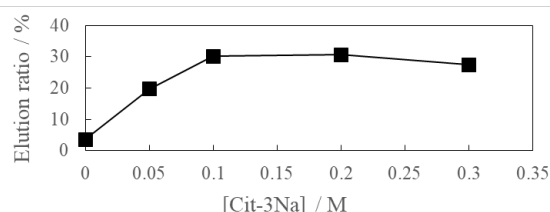

Fig. 3.   dependence of Cit-3Na concentration on elution ratio of Re(VII).

REFERENCES:
[1] M. G. B. Drew *et al.*, Dalton Trans. (2007) 244-251.
[2] Y. Yoshimura *et al.*, KURRI Progress Report 2019 (2020).

R2P7-5

PR4-4 Consistency verification between relativistic quantum chemical calculations and experiments in uranium compounds

M. Abe[1,2], M. Hada[2], A. Sato[2], A. Yoshida[2], T. Yamamura[2], A. Sunaga[3], C. Tabata[3]

[1]*Department of Chemistry, Hiroshima University*
[2]*Department of Chemistry, Tokyo Metropolitan University*
[3]*Institute for Integrated Radiation and Nuclear Science, Kyoto University*

INTRODUCTION: Theoretical calculations of actinide compounds are very important to understand or predict new phenomenon in these compounds. We have developed computational methods based on relativistic quantum chemistry, which can describe electronic states of actinide compounds. In this work, we calculated equilibrium isotope fractionation coefficients (ε) for 64 U species in U(VI), U(V), and U(IV) states with various ligands (e.g., H_2O, CO_3^{2-}, CH_3COO^-, Cl^-, NO_3^-, etc.) using accurate relativistic quantum chemical methods. The U isotope fractionations are important and widely discussed in geochemistry [1]. We verify the accuracy of the computational methods by comparing to some experimental results of U isotope fractionations.

METHODS: We calculated ε between ^{235}U and ^{238}U as the sum of the nuclear volume term ($\ln K_{nv}$) and the nuclear mass term ($\ln K_{nm}$) [2-4]. $\ln K_{nv}$ is due to the electronic energy difference caused by the different size and shape of nucleus of isotopes [2,3], while $\ln K_{nm}$ is due to the vibrational level caused by the different reduced mass of isotopologues [4]. In the heavy element system, $\ln K_{nv}$ is dominant in ε. Because $\ln K_{nv}$ is highly affected by relativity, we used the exact two-component (X2C) relativistic method with the Gaussian finite nucleus model, implemented in the DIRAC16 program. We performed both the Hartree-Fock (HF) and density functional theory calculations using the B3LYP functional to discuss the electron correlation effects in $\ln K_{nv}$.

RESULTS: Fig. 1 (a) and (b) show the calculated results, and the magnitude of ε obtained is approximately U(VI) > U(V) > U(IV) for both the HF and DFT cases. The ε values between U(VI)-U(IV) were obtained in the range of 0.96~3.00‰ for X2C-HF, and 0.53~1.94‰ for X2C-B3LYP; thus, the results between HF and DFT are different. The equilibrium ε between U(VI)-U(IV) in hydrochloric acid was estimated as 1.70‰ from X2C-HF and 0.92‰ from X2C-B3LYP, while the experimental counterpart was reported as 1.64‰ [5]. Therefore, the X2C-HF method seems to be more reliable for the ε calculation between U(VI)-U(IV).

On the other hand, if we consider the isotope fractionations in the U(VI)-U(VI) ligand exchange systems, the ε values obtained at the DFT level show generally better agreements with experiments [6,7] than those for HF. This indicates that the DFT calculations are accurate for U(VI) species, which are closed-shell systems, but not for

U(IV) species, which are open-shell systems. Recently, we found that the DFT calculations in the DRAC program do not automatically adopt the average-of-configuration (AOC) open-shell algorithm, whereas our HF calculations adopt it. Hence, recalculations including AOC for DFT is ongoing to improve the description for the open-shell U(IV) electronic states.
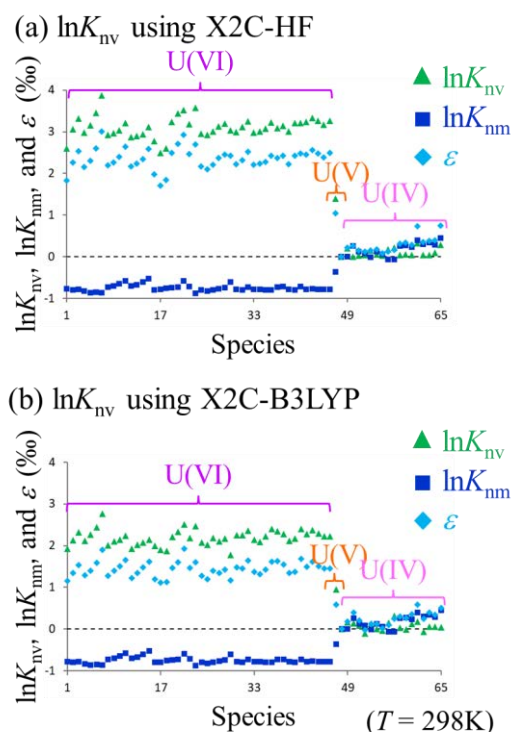

Fig. 1. $\ln K_{nv}$, $\ln K_{nm}$, and ε of 64 U species, calculated (a) at the HF level and (b) at the B3LYP levels for $\ln K_{nv}$. The light blue, green, and deep blue plots represent ε, $\ln K_{nv}$, and $\ln K_{nm}$, respectively. These plots for U(VI), U(V), and U(IV) species are surrounded by the purple, orange, and pink rounded squares, respectively. [8]

REFERENCES:
[1] C. H. Stirling *et al.*, Geochim. Cosmochim. Acta, **163** (2015) 200-218.
[2] M. Nomura *et al.*, J. Am. Chem. Soc., **118** (1996) 9127-9130.
[3] J. Bigeleisen, J. Am. Chem. Soc., **118** (1996) 3676-3680.
[4] J. Bigeleisen and M. G. Mayer, J. Chem. Phys., **15** (1947) 261-267.
[5] Wang *et al*. Geochim. Cosmochim. Acta, **158**, 262 (2015)
[6] Kim *et al*. J. Chem. Phys. **81**, 6266 (1984).
[7] Aoyama *et al*. J. Phys. Chem., **93**, 2666 (1989).
[8] A. Sato, R. Bernier-Latmani, M. Hada, and M. Abe, to be submitted.

R2P7-6

PR4-5   Evaluation of Phase Diagram of Minor Actinide Oxides with CALPHAD

H. Shishido, H. Hashizume, C. Tabata[1], T. Yamamura[1]

Graduate School of Engineering, Tohoku University

[1]*Institute for Integrated Radiation and Nuclear Science, Kyoto University*

INTRODUCTION: Partitioning and transmuting is presently regarded as an effective method to address the issue of high-level radioactive waste disposal [1]. We have proposed to transmute MA rather moderately, namely with a low fission reaction rate to avoid imposing severe engineering challenges on the system design [2]. This concept has considered MA mixed oxides (e.g., Np–Am–O) to be loaded into limited space in fusion re-actors. Whereas some studies have reported the phase diagram of U or Pu based MA oxides, no reports have provided the diagrams of the MA-only mixed oxides.

The objective of this study is to evaluate the ther-modynamic values and phase diagram of the MA-only mixed oxides. Measurement of the phase diagrams is not a straightforward task; we thus aim to develop a method to evaluate the phase diagrams.

In the current fiscal year, we have performed the electronic structure calculations of NpO_2 and AmO_2 mixed oxide based on the method obtained in the previ-ous year. Because there are no reported crystal structure data for the mixed oxide, crystal structures were prepared assuming appropriate atomic configurations, and struc-tural optimization calculations were performed on them.

METHODS: The calculated crystal structure of (Np, Am)O_2 is shown in Fig. 1. The composition ratio of Np to Am is 1:1, and the atomic arrangement of Np and Am is assumed to have the two crystal structures shown in Fig. 1. The crystal groups are P4/mmm and R-3m, respec-tively. We performed the structural optimization for these crystals. We used WIEN2k to calculate the electronic state [3]. The generalized gradient approximation (GGA) developed by Perdew, Burke, and Ernzerhof was used as the exchange–correlation functional. The product of the muffin-tin radius and the K vector ($R_{mt}K_{max}$) was 8.5 Ry, and the sampling k points were set to 5,000. The calcula-tion was performed as a non-magnetic material without considering the matters related to the electron spin.

RESULTS: The Energy–Volume curves for the two crystal structures of (Np, Am)O_2 are shown in Fig. 2. The curves show Murnaghan's fitting curves. Whereas there is no significant difference between the two crystal struc-tures, the total energy is slightly lower for the R-3m crystal structure.

REFERENCES:
[1] S. L. Beaman *et al.*, NR-CONF-001, United States Nuclear Regulatory Commission, (1976).
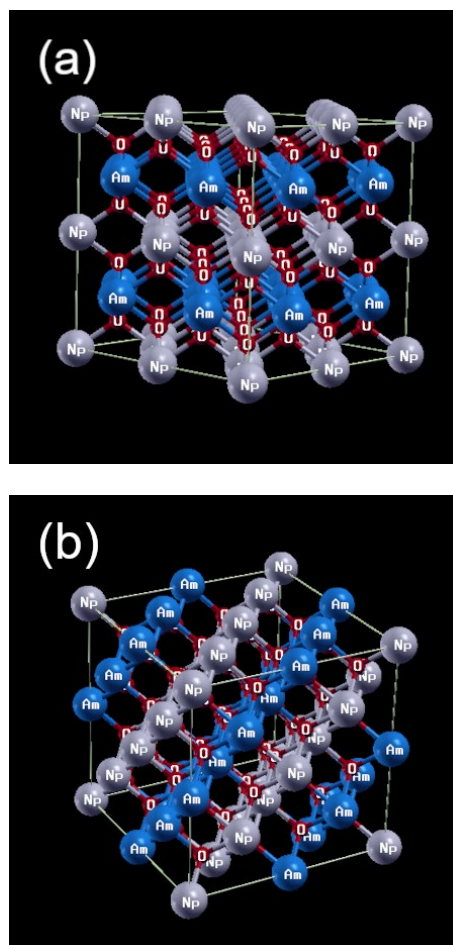[2] Y. Furudate *et al.*, Prog. Nucl. Energ. **103** (2018) 28-32.

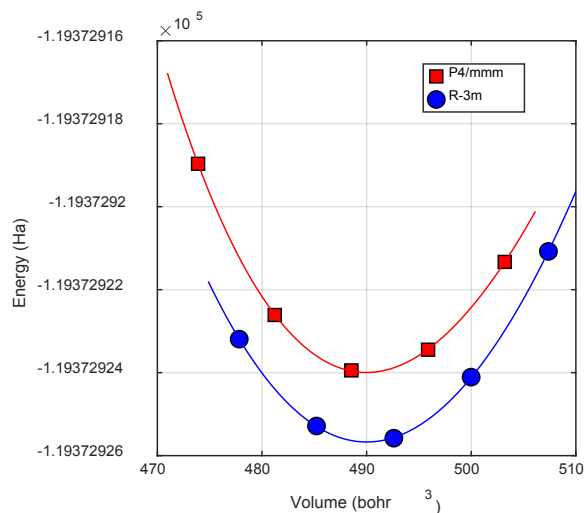Fig. 1.   Crystal structure of (Np, Am)O_2: (a) P4/mmm; (b) R-3m.

Fig.2.   Energy volume curve of (Np, Am)O_2.

[3] P. Blaha, K.Schwarz *et al.*, J. Chem. Phys. **152** (2020) 074101.

R2P7-7

PR4-6 Peculiar magnetism in uranium intermetallics with layered structure

Y. Haga[1], C. Tabata[2] and Y. Matsumoto[3]

[1]Advanced Science Research Center, JAEA
[2]Institute for Integrated Radiation and Nuclear Science, Kyoto University
[3]Faculty of Science, Toyama University

INTRODUCTION: Unusual physical properties arising from geometrical characteristics of magnetic moments are now attracting active research interests. In particular, the situations where magnetic interactions are frustrating can result in highly unconventional ground states as demonstrated historically by the spin-glass or, more recently, skyrmions formations involving a number of spins. Here, we investigate uranium compounds where the uranium atoms form honeycomb layers. The target materials in this study are a series of compounds having $Sr_{0.6}Fe_2Si_{4.9}$-type structure where uranium atoms are located at Sr position. Although earlier study suggested atomic disorder inside the uranium layer, our investigation on a U-Pt-Ga ternary analogue showed that a honeycomb arrangement of uranium atoms is likely. The resulting formula should therefore be $U_2Pt_6Ga_{15}$. In this study we further investigated uranium intermetallics with the same crystal structure.

EXPERIMENTS: Single crystals were grown from the self-flux method. The chemical composition of the samples was characterized by the electron-probe microanalysis. Crystal structure was determined using the single-crystal X-ray diffraction.

RESULTS: We have successfully grown single crystals of $U_2Pt_6Al_{15}$ [2] and $U_2Pt_6Ga_{15}$[3]. Reflecting the different atomic radius of Al and Ga, the lattice parameters of these compounds differ as shown in Table 1. The reduction of the lattice parameters would modify the electronic interaction through the change in the interatomic distances. In f-electron system in general, the smaller the interatomic distance increases the hybridization and leads to a modification of magnetic interaction. Considering the same valence electron count in Al and Ga, the substitution effect would result primarily in chemical pressure effect.

Temperature dependence of magnetization divided by magnetic field applied along the c-direction is shown in Fig. 1 for both $U_2Pt_6Al_{15}$ and $U_2Pt_6Ga_{15}$. Both compounds show an anomaly in M/H corresponding to the magnetic phase transition at around 25 K as shown by arrows in Fig. 1.
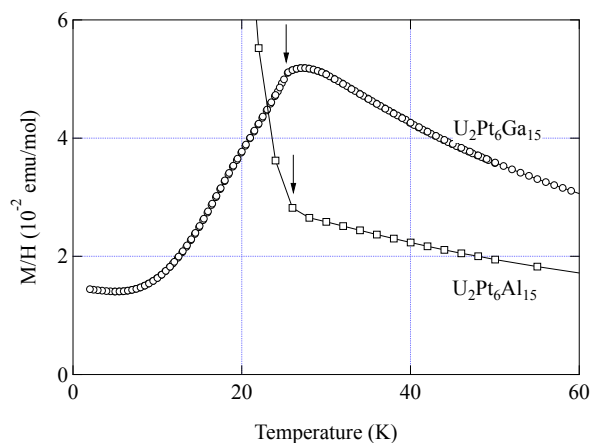

Figure 1. Temperature dependence of magnetization divided by magnetic field for $U_2Pt_6Al_{15}$ and $U_2Pt_6Ga_{15}$.

This result demonstrates that the magnetic properties are drastically modified by substituting Al to Ga. Although the transition temperature is almost the same, the low temperature behavior is completely different. While $U_2Pt_6Ga_{15}$ shows a typical antiferromagnetic behavior, $U_2Pt_6Al_{15}$ shows a steep enhancement of magnetization in the ordered state. Detailed investigation on $U_2Pt_6Al_{15}$ (not shown) further suggests existence of multiple magnetically ordered phases as functions of temperature and magnetic field, which cannot be explained by a simple antiferromagnetic ordering.

Present results demonstrate that uranium layers embedded in the metallic Pt-Al(Ga) block show a variety of magnetic characteristics.

REFERENCES:
[1] Y. Haga *et al.*, JPS Conf. Ser., **29** (2020) 013003-1-5.
[2] Y. Matsumoto, Y. Haga *et al.*, J. Phys. Soc. Jpn. **90**, 074707 (2021).

	a (Å)	c (Å)
$U_2Pt_6Al_{15}$	4.2957(7)	16.2211(14)
$U_2Pt_6Ga_{15}$	4.3038(5)	16.297(2)

Table. 1. Lattice parameters of $U_2Pt_6Al_{15}$ and $U_2Pt_6Ga_{15}$.

R3P4-1

PR4-7　Adsortpion Chracterization of Actinide Chemical Species on Solid Adsorbents

T. Suzuki[1], F. Yin[1], R. Murayama[1], S. Fukutani[2], A. Sunaga[2], C. Tabata[2] and T. Yamamura[2]

[1]*Department of Nuclear System Safety Engineering, Ngaoka University of Technology*
[2]*Institute for Integrated Radiation and Nuclear Science, Kyoto University*

INTRODUCTION: We have been studying the solid adsorbents for separation and recovery of actinides [1], and actinide analysis [2]. Recently, the supply of α-nuclides for α-therapy is becoming increasingly important. For the purpose, the actinides separation from the decay series is required. In this year, the adsorption behaviors of actinides on polyvinylpolypyrrolidone (PVPP) and styrene (Sty)-divinylbenzene (DVB) type pyrrolidone resin were investigated. Especially, we obtained the extended data about adsorption of thorium ion on PVPP, and investigated the cross-linkage effects on the adsorption. In addition, we studied the dissolution methods of thoria.

EXPERIMENTS: We used the commercially available type PVPP (Alfa Aesar) and synthesized pyrrolidone resin in our laboratory. The synthesized resins are N-vinylpyrrolidone (VP)/ Sty/DVB copolymers. These resins were synthesized with the different mixing ratio of monomers by the bulk -polymerization method. The proportion of DVB and total monomer is same to cross-linkage degree. The thorium ion was used in ICP-MS standard solution (XSTC-311, SPEX) and uranyl ion was used in XSTC-289. The adsorption behaviors were discussed by using distribution coefficient, Kd [mL/g]. Kds were obtained by batch experiment.

RESULTS: The adsorption behavior of thorium ion in HNO_3 solution is shown in Fig.2. We confirmed that the thorium is strongly adsorbed on PVPP in higher concentration of HNO_3, while thorium is weekly adsorbed in lower concentration of HNO_3. The results of the dependence of adsorption on the mixing ratio of monomers are shown in Fig. 2. Percentage of DVB means the cross-linkage degree. Kds are standardized by percentage of VP. We confirmed the cross-linkage effects on adsorption of uranyl ion on pyrrolidone resin in HNO_3 solution. The difference of adsorption behaviors by VP-ratio can be explained by the difference of permittivity and hydrophobicity of resins. The normalized distribution coefficient increases or decreases depending on cross-linkage degree in the case of constant VP percentages. The adsorption tendency is varied between the VP percentage of 70% and 60%. We found that this tendency change is related with the surface potential of resin. However, the mechanism of surface potential change is not clarified, although we infer this effect due to the swelling-shrinking tendency of resin [3].
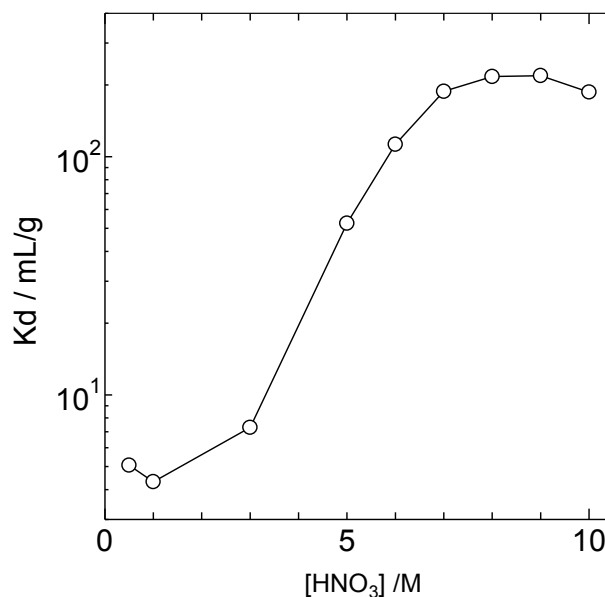

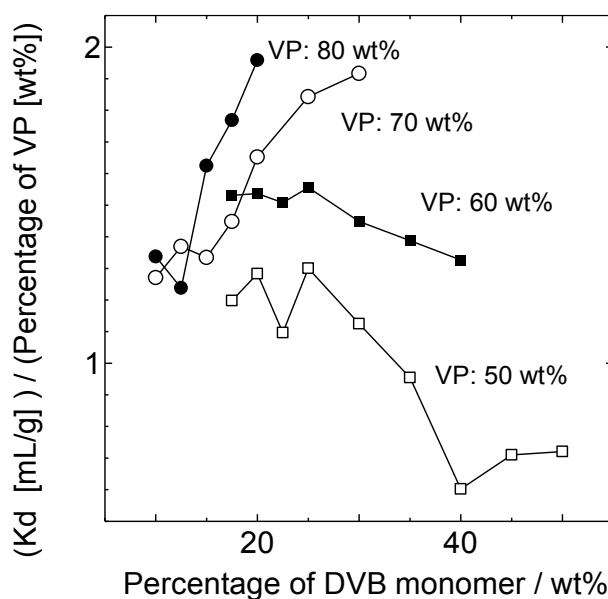Fig. 1.　Adsorption behavior of thorium ion on PVPP in HNO_3 solution.

Fig. 2.　Cross-linkage effects on adsorption of uranyl ion on pyrrolidone resin in HNO_3 solution.

REFERENCES:
[1] 鈴木達也, 日本イオン交換学会誌, 30 (2019) 33-38.
[2] T. Suzuki, *et al.* J. Radioanal. Nucl. Chem., 318 (2018) 221-225.
[3] T. Yamamizu,*et al*., Jpn. J. Polymer Sci. Technol., 47 (1990)49-56. (in Japanese)

R3P4-2

PR4-8   A Study on Effect of Polymer Network on Resins for Separating Actinyl Ions

M. Nogami[1], C. Tabata[2], M. Yokota[1], H. Kita[1], and T. Yamamura[2]

[1]*Faculty of Science and Engineering, Kindai University*
[2]*Institute for Integrated Radiation and Nuclear Science, Kyoto University*

INTRODUCTION: Development of highly selective compounds for actinyl ions in aqueous media (extractants, precipitants, resins, etc.) has been important. We have been focusing on monoamide compounds (Fig. 1) as promising candidates for nitric acid media, considering the possibility of complete incineration of waste compounds (so-called "CHON principle"[1]). For the resins, we have taken two factors into accounts for selective interaction between functional monoamide groups and actinyl ions; one is "chelating effect" of the ring formed by polymer monoamides and actinyl ion(s), and the other is "flexibility" of monoamide. Our previous experimental results suggest that the contribution of "chelating effect" is predominant. This report describes our past one year's activity in the above research field.

Fig. 1.   Chemical structure of monoamide compounds
(R, R', R" : hydrocarbon group)

RESULTS: We made fruitful discussions with other research groups especially through symposiums organized by IIRNS. For developing our resins, we have devoted our attention to the interaction between functional monoamide groups and actinyl ions as described above. However, we were given a comment on the importance of "component except functional monoamide groups", namely, "chemical structure of polymer network" in the resin. In our resins, divinylbenzene (DVB) is basically used as the crosslinking agent. Also, many resins with a longer chain between the functional monoamide group and the main polymer chain consist of derivatives of polychloromethylstyrene. The point of the comment was that the benzene ring included in the above-described compounds might decrease adsorptivity to metal ions, and that, therefore, it would be worth trying for us to newly synthesize resins without benzene rings as the component.

For the suggestion, we have already partially tried. Diethyleneglycoldimethacrylate (DEGDMA : Fig. 2) was used as a crosslinking agent except DVB. DEGDMA consists of methacrylate ester and ether, and has no benzene rings as can be seen. In the earlier study in the field of actinide chemistry by another research group, such crosslinking agents as methacrylate ester system have been investigated for application to those for suspension polymerization of amidoxime resin (Fig. 3) which is well known as the resin for recovery of U from seawater. According to the literature, by mixing one of

these methacrylate esters with DVB, improvement of adsorption capacity and rate have been found compared with the case where only DVB was used as the crosslinking agent. It is basically because addition of methacrylate ester compounds increases hydrophilicity of resins. On the contrary, mechanical strength and acid/base resistance has been found decreased[2].
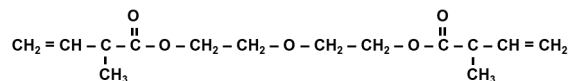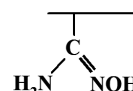

Fig. 2.   Chemical structure of DEGDMA

Fig. 3.   Chemical structure of amidoxime resin

In our research on crosslinking agents, we synthesized "diamide" resin, not monoamide one, by similarly using the mixture of DEGDMA and DVB. Diamide compounds are famous for the separation of actinide(III) and lanthanide(III) species as well as actinide(IV) and (VI) ones[3]. The applied functional diamide compound was *N,N,N',N'*- tetramethylmalonamide (TMMA : Fig. 4) and the resin was derived from polychloromethylstyrene like monoamide resins with a longer chain. The "TMMA resin" was examined for a column adsorption/elution experiment using Nd(III) under the following conditions ; column : 8 mmφ x 50 mmH, packed resin volume : 2.5 cm^3, feed solution : 3 mol/dm^3 (=M) HNO$_3$ containing 10 mM Nd(III), eluent : 0.05 M HNO$_3$, temperature : 50 ^{o}C, SV : 24 h^{-1}. As the result, a distinguished tendency was obtained from the elution experiment. Namely, only ca. 38 % of adsorbed Nd(III) was eluted against our expectation of almost 100 % elution. This strongly suggests that esters in DEGDMA underwent acid hydrolysis followed by the formation of carboxyl and hydroxyl groups which have adsorptivity under low HNO$_3$ concentration of 0.05 M. Considering the above, applicability of compounds with esters to the component of monoamide resins would be difficult due to unstable characteristics under relatively higher concentration of HNO$_3$.
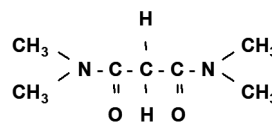

Fig. 4.   Chemical structure of TMMA

REFERENCES:
[1] M. G. B. Drew *et al.*, Dalton Trans. (2007) 244-251.
[2] H. Egawa *et al.*, J. Atomic Energy Soc. Jpn., **29** (1987) 1079-1086 (In Japanese).
[3] C. Madic *et al.*, *European Report, EUR19149*; European Commission: Brussels (2000) 9-82.

R3P4-3

PR4-9   XAFS study on the aged deterioration of a simulated fuel debris

T. Kobayashi[1], T. Yaita[1], C. Tabata[2], T. Kubota[3], T. Yamamura[2]

[1]Materials Sciences Research Center, Japan Atomic Energy Agency
[2]Institute for Integrated Radiation and Nuclear Science, Kyoto University
[3]Agency for Health, Safety and Environment, Kyoto University

INTRODUCTION: For decommissioning the Fukushima-Daiichi Nuclear Power Plant, it is necessary to understand the characteristics of fuel debris. Particularly, for safe and reliable removing of the debris, estimation of the aged deterioration of a debris with changes in environmental conditions could be required. Thus, this study is aiming to investigate the changes in chemical state and structure of a simulated fuel debris under controlled environment simulating conditions inside and/or outside the reactor by XAFS method.

EXPERIMENTS: Currently, the fuel debris inside the reactor is expected to be placed in a high radiation environment and reductive atmosphere while being immersed in water. Thus, in this study, a simulated debris samples prepared by sintering UO_2 and ZrO_2 was immersed in water and the samples were irradiated with γ-ray to simulate the high radiation environment inside the reactor. The samples were prepared at Nuclear Science Research Institute of JAEA and Hot Laboratory of Institute for Integrated Radiation and Nuclear Science, Kyoto University. The γ-ray irradiation was performed at LINAC of Institute for Integrated Radiation and Nuclear Science, Kyoto University. The XAFS measurement was performed at JAEA beamline BL22XU of SPring-8.

RESULTS: As a result, it was found that the uranium on the surface of the sample was oxidized from tetravalent to hexavalent and the U-O distance was shortened, by immersing samples in water and irradiating it with γ-rays (Fig. 1). From the comparison of the samples in which the immersion time and the γ irradiation time were varied, it was revealed that the oxidation reaction mainly occurred during the γ-ray irradiation. Furthermore, even if the sample was picked out from water and exposed to the air atmosphere, no change was observed in the valence or local structure of uranium, suggesting that debris may be stable in the atmosphere.
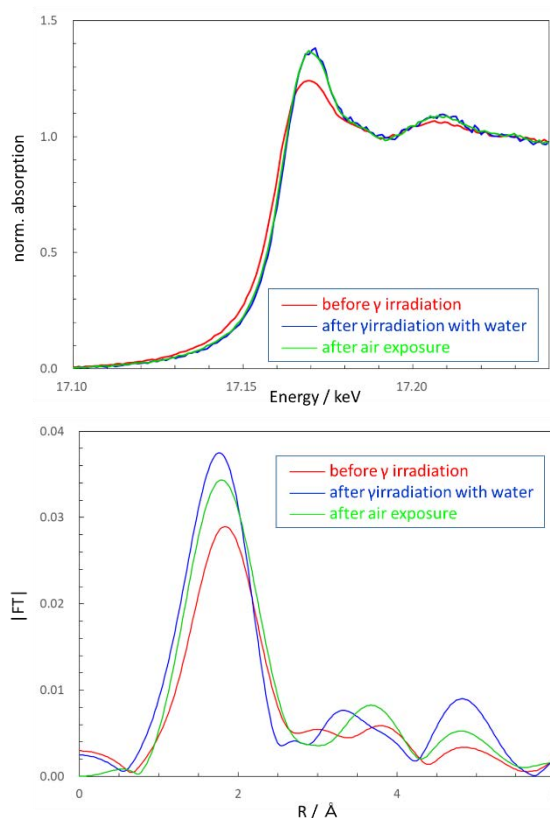

Fig. 1 XANES spectra (upper) and radial structure functions (lower) of simulated fuel debris under several conditions.

R3P4-4

PR4-10 Synthesis of nobel phthaloyanine derivatives and effect of substitutent on recognition of light actinide and chemical property-3

M. Nakase[1], M. Harigai[1], C. Tabata[2], T. Yamamura[2]

[1]Institute of Innovative Research, Tokyo Institute of Technology
[2]Institute for Integrated Radiation and Nuclear Science, Kyoto University

INTRODUCTION: Effective separation of U from Th and other fission products in spent Th fuels is needed in Th fuel cycle. To enable the separation, thorium–uranium extraction (THOREX) process, like the plutonium–uranium redox extraction (PUREX) process, has been studied [1]. In the THOREX process, UO_2^{2+} is extracted by tri-*n*-butyl phosphate (TBP) with the aid of $Al(NO_3)_3$. Some of the other extractant which consisted of C, H, O, N atoms (CHON principle) such as monoamide is recently reported for U/Th separation [2]. In this study, Phthalocyanine (Pc) was selected as the main structure of the extractant which also satisfy the CHON principle. To make the solubility of Pc in organic solvent higher, the Pc derivatization is ongoing. The Pc-metal complex in organic solvent itself is interesting to investigate. To obtain the complex with actinide, the purification technique with minimized waste production is highly desirable. In FY2021, some of the purification techniques were tested including chromatography, Solxlet extraction and sublimation. This year, some of the purified samples, mainly Pc-Zn compounds were characterized as well as the other samples.

EXPERIMENTS: The Pc-Zn complex was purified by sublimation by the hand-made apparatus equipped last year as shown in **Figure 1**. The pure product was supposed to be solid (powder), but the obtained product was slightly wet maybe due to the moisture in the air since the Pc-Zn sample was exposed in the hot temperature. By the ^{1}H-NMR, judgement of purification condition was difficult due to the similarity of the Pc and the substructure of Pc such as phthalonitrile. Therefore, powder x-ray diffraction (PXRD) and Raman spectrophotometry were implemented as well as further purification test. The Laser Raman Spectrophotometer (NRS-3100) is shown in Figure 3
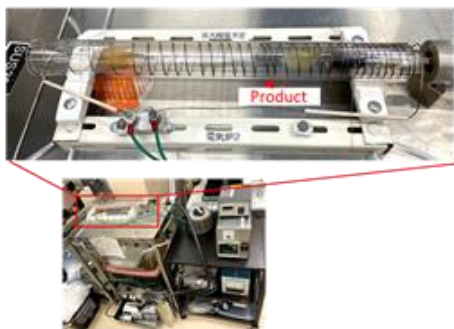

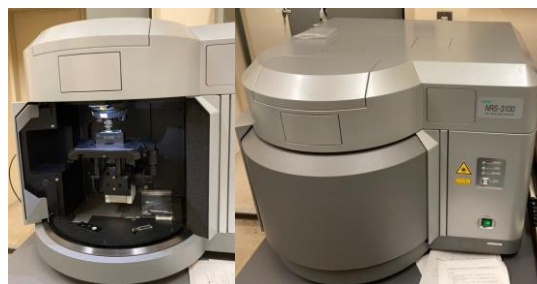Figure 1 Sublimation setup equipped at Kyoto University.

Figure 2 Laser Raman Spectrophotometer (NRS-3100) .

RESULTS: The Purified Pc-Zn sample and its XRD pattern are shown in Figure 3 and 4. In the XRD pattern, large hallow peak was seen due to the use of ethanol and glass plate, but some of the sharp diffraction attributed to Pc are seen. Therefore, we decide that the purification by sublimation was successful. The Raman spectra in good quality was also obtained and the evaluation by database is ongoing. Raman spectra of other phosphate samples (simulated waste generated in Fukushima Daiichi nuclear Power Station, synthesized in Tokyo Tech) were also measured properly. Due to the strong laser, it seems that the sealed samples can also be measured by adjusting the measurement conditions.
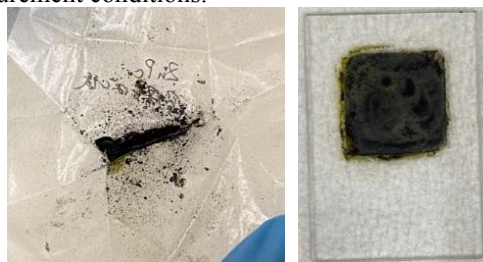

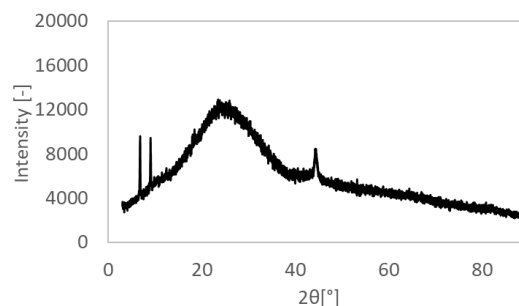Figure 3 Purified Pc-Zn (left; after sublimination, right; Pc-Zn spread by ethanol for PXRD) .

Figure 4 PXRD pattern of sublimated Pc-Zn.

PLANS: We accelerate the synthesis of Pc derivatives and Pc-Actinide complex in both solid and in solution in next year. In addition, some of the irradiated samples such as phosphate waste forms will be shipped to Kyoto University for further characterization.

REFERENCES:

[1] R.H.Rainey and J.G.Moore, *Nucl Sci Eng*, 10(4), 367–371, 1961.
[2] P.N.Pathak, *Solv Ext Ion Exch*, 20(3), 293–311, 2002.

R3P4-5